Citation: Molecular Therapy–Nucleic Acids (2012) 1, e62; doi:10.1038/mtna.2012.54

www.nature.com/mtna

Dual Myostatin and Dystrophin Exon Skipping by Morpholino Nucleic Acid Oligomers Conjugated to a Cell-penetrating Peptide Is a Promising Therapeutic Strategy for the Treatment of Duchenne Muscular Dystrophy

Alberto Malerba[1,2], Jagjeet K Kang[1], Graham McClorey[3], Amer F Saleh[4], Linda Popplewell[1], Michael J Gait[4], Matthew JA Wood[3] and George Dickson[1]

The knockdown of myostatin, a negative regulator of skeletal muscle mass may have important implications in disease conditions accompanied by muscle mass loss like cancer, HIV/AIDS, sarcopenia, muscle atrophy, and Duchenne muscular dystrophy (DMD). In DMD patients, where major muscle loss has occurred due to a lack of dystrophin, the therapeutic restoration of dystrophin expression alone in older patients may not be sufficient to restore the functionality of the muscles. We recently demonstrated that phosphorodiamidate morpholino oligomers (PMOs) can be used to re-direct myostatin splicing and promote the expression of an out-of-frame transcript so reducing the amount of the synthesized myostatin protein. Furthermore, the systemic administration of the same PMO conjugated to an octaguanidine moiety (Vivo-PMO) led to a significant increase in the mass of soleus muscle of treated mice. Here, we have further optimized the use of Vivo-PMO in normal mice and also tested the efficacy of the same PMO conjugated to an arginine-rich cell-penetrating peptide (B-PMO). Similar experiments conducted in mdx dystrophic mice showed that B-PMO targeting myostatin is able to significantly increase the tibialis anterior (TA) muscle weight and when coadministered with a B-PMO targeting the dystrophin exon 23, it does not have a detrimental interaction. This study confirms that myostatin knockdown by exon skipping is a potential therapeutic strategy to counteract muscle wasting conditions and dual myostatin and dystrophin skipping has potential as a therapy for DMD.

Molecular Therapy–Nucleic Acids (2012) **1**, e62; doi:10.1038/mtna.2012.54; published online 18 December 2012
Subject Category: Nucleic acid chemistries, Antisense oligonucleotides

Introduction

Myostatin, a transforming growth factor-β family member, is a negative regulator of skeletal muscle mass[1] and several approaches have been used to knockdown this protein to induce an increase in skeletal muscle growth.[2] This could have important implications in disease conditions including cancer and HIV/AIDS, which are accompanied by muscle mass loss. Sarcopenia, muscle atrophy, obesity-related metabolic disorders, and insulin resistance may potentially also be ameliorated by inducing myostatin inhibition. In the context of Duchenne muscular dystrophy (DMD), although dystrophin restoration can be achieved using different approaches including overexpression of mini/microdystrophin and dystrophin exon skipping, it is likely to be less effective if the disease has already progressed to a state where there is advanced muscle wasting and damage. Blockade of myostatin activity could therefore have a therapeutic effect in DMD. As myostatin has conserved function in humans, it is likely that muscle regeneration resulting from myostatin inhibition in animal models can be reproduced in humans. Inhibition of intracellular signal transduction, blockade of extracellular activity of myostatin, and decrease in signaling of myostatin have been explored for inhibiting myostatin expression. Myostatin neutralizing antibody was prepared by immunizing myostatin-null mice with recombinant myostatin and its treatment resulted in improved muscle mass and function in preclinical studies.[3] The clinical trial of a monoclonal neutralizing antibody to myostatin, MYO-029, established a good safety profile, but no improvement in muscle function or strength was observed.[4] A modified myostatin propeptide that is resistant to proteolytic cleavage has been shown to bind myostatin and inhibit its signal transduction, resulting in an increase in skeletal muscle weight in animal studies.[5,6] Follistatin, a secreted glycoprotein that binds very strongly to myostatin, has been used to induce muscle mass growth. However, its inhibitory effects are not specific to myostatin suggesting that it also inhibits other transforming growth factor-β family members during muscle growth.[7] In fact, myostatin inhibition in animal models by ACE-031, a soluble form of activin receptor type IIb (AcRIIb) showed a significant increase in muscle mass, independent of fiber type.[8] The use of antisense oligonucleotides (AOs) to induce exon skipping and thereby knockdown the expression of myostatin presents several advantages over the other currently used gene therapy approaches. First, there is no risk of uncontrolled insertion into the genome with AOs, as is the case for virus-mediated approaches.[9] Moreover,

The first three authors contributed equally to this study.
[1]School of Biological Sciences, Royal Holloway, University of London, Surrey, UK; [2]Department of Veterinary basic sciences, Royal Veterinary College, London, UK; [3]Department of Physiology, Anatomy and Genetics, University of Oxford, Oxford, UK; [4]Medical Research Council Laboratory of Molecular Biology, Cambridge, UK. Correspondence: George Dickson, School of Biological Sciences, Royal Holloway—University of London, Egham, Surrey, TW20 0EX, UK. E-mail: G.Dickson@rhul.ac.uk
Keywords: antisense oligonucleotides; Duchenne muscular dystrophy; dystrophin; exon skipping; myostatin
Received 7 August 2012; accepted 15 October 2012; advance online publication 18 December 2012. doi:10.1038/mtna.2012.54

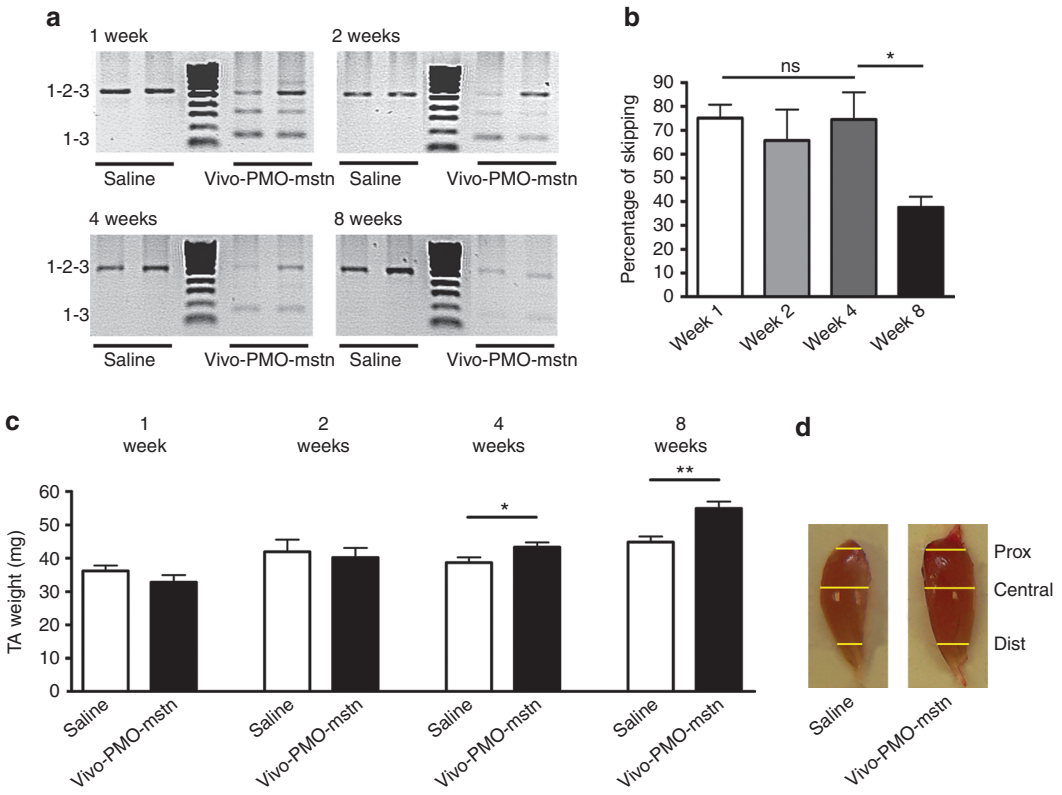

Figure 1 Single intramuscular injection of Vivo-PMO-mstn in C57BL10 mice increases muscle mass. Vivo-PMO-mstn (10 µg) was injected into the left tibialis anterior (TA) of C57BL10 mice ($n = 6$). The contralateral muscle was injected with excipient. Mice were killed after 1, 2, 4, and 8 weeks. (**a**) Representative products of nested RT-PCR analysis of myostatin exon 2 skipping in treated and control muscles at 1, 2, 4 or 8 weeks after the injection are shown. (**b**) Densitometric analyses of nested RT-PCR products of myostatin exon 2 skipping in treated and control muscles at 1, 2, 4 or 8 weeks ($n = 6$). Levels of exon skipping declined 8 weeks after the injection. Both bands corresponding to skipped products were included in the analysis. (**c**) Change in TA muscle mass following a single intramuscular injection of Vivo-PMO-mstn after 1, 2, 4 or 8 weeks. (Two-tailed *t*-test, $^{*}P = 0.0404$; $^{**}P = 0.005$, $n = 6$). (**d**) Representative TA muscles collected 8 weeks after a single injection of saline (left) or Vivo-PMO-mstn (right). Proximal (prox), central (central), and distal (dist) levels of the muscles are indicated by yellow lines. ns, not significant; PMO, phosphorodiamidate morpholino oligomer; RT-PCR, reverse transcription-PCR.

with an appropriate dosing regimen, exon-skipping levels can be regulated and, if necessary, the treatment can be interrupted.[10] Importantly, antisense phosphorodiamidate morpholino oligomers (PMOs) have not been reported to produce any toxic effects or immune response so far in animal models, as well as when used in clinical application.[11] We published the proof of principle that myostatin knockdown can be obtained by using octaguanidine-conjugated PMOs (Vivo-PMOs) to skip the out-of-frame exon 2 of the pre-mRNA and so inducing hypertrophy in the skeletal muscle of normal healthy mice.[12] Recently, the same strategy combining dystrophin restoration and myostatin inhibition by dual exon skipping has been reported in DMD muscle cells in culture using 2′-O-methyl-phosphorothioate (2′OMePS) RNA AOs. Dual skipping of dystrophin and myostatin exon 2 was demonstrated to be feasible in mouse and human cells with no interference between the two AOs. However, the skipping levels seen with these 2′OMePS AOs were low, and conclusions of applicability of dual exon skipping as an *in vivo* treatment for dystrophin deficiency could not be drawn.[13] To improve the efficacy of the dual dystrophin and myostatin exon-skipping strategy, in this study we have again used the alternative PMO chemistry that has been reported have better efficacy.[14] Furthermore, we have determined the efficacy of dual exon skipping of myostatin (exon 2) and dystrophin (exon 23) with PMOs conjugated with a cell-penetrating peptide[15] and administered simultaneously in mdx mice. The study shows that antisense-mediated destructive exon skipping of myostatin has great potential to be a part of a combination therapy alongside antisense-mediated reframing and restoration of dystrophin expression in the treatment of DMD.

Results

Myostatin knockdown after single Vivo-PMO intramuscular administration induces significant increase in muscle mass

Before verifying the efficacy of a cell-penetrating peptide-conjugated PMO (B-PMO), we established the persistence of myostatin knockdown induced by PMO administration by using the previously tested octaguanidine-conjugated form of the 28-mer PMO-D (called in this manuscript as PMO-mstn for clarity). Wild-type female mice (6-week-old C57BL10 mice, $n = 24$) were injected in the tibialis anterior (TA) with a single intramuscular injection of 10 µg of Vivo-PMO-mstn. Contralateral TA muscles were injected with same volume of saline as

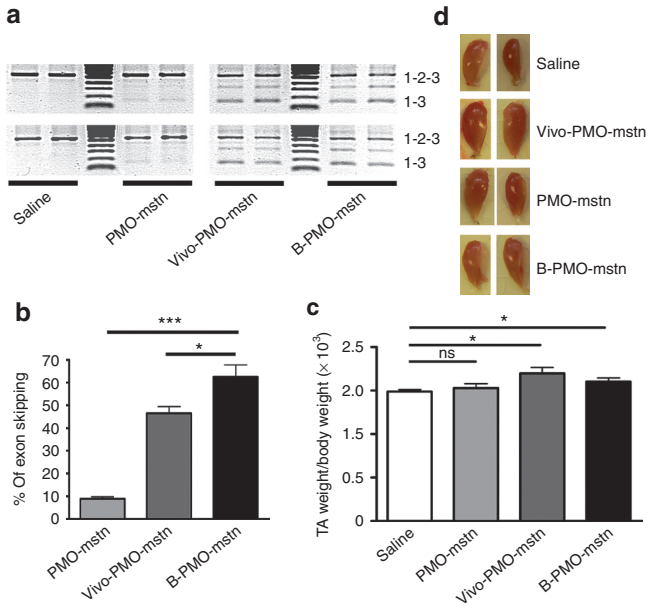

Figure 2 Single intramuscular injection of PMO-mstn linked to an arginine-rich cell-penetrating peptide in C57BL10 mice increases muscle mass. Tibialis anterior (TA) muscles of C57BL10 mice were treated with 10 µg of unconjugated PMO-mstn, Vivo-PMO-mstn, B-PMO-mstn or excipient ($n = 6$). Mice were killed after 8 weeks and nested RT-PCR was performed on treated and control muscle RNAs. (**a**) Representative products of nested RT-PCR analysis of myostatin exon 2 skipping from muscles treated with the different PMOs are shown. (**b**) Densitometric analyses of nested RT-PCR products for percentage of myostatin exon 2 skipping in treated and control muscles. A statistically significant difference was observed in exon skipping mediated by B-PMO-mstn compared with both Vivo-PMO-mstn and unconjugated PMO (*$P = 0.02$ and ***$P < 0.0001$ respectively, two-tailed *t*-test, $n = 6$). Both bands corresponding to skipped products were included in the analysis. (**c**) Change of mass in treated and control muscles. Both B-PMO-mstn ($P = 0.04$) and Vivo-PMO-mstn ($P = 0.01$) treated muscles were significantly heavier than control muscles (two tailed *t*-test, *$P < 0.05$ and ***$P < 0.001$, $n = 6$). (**d**) Representative TA muscles collected 8 weeks after treatment with the different PMOs or with excipient. ns, not significant; PMO, phosphorodiamidate morpholino oligomer; RT-PCR, reverse transcription-PCR.

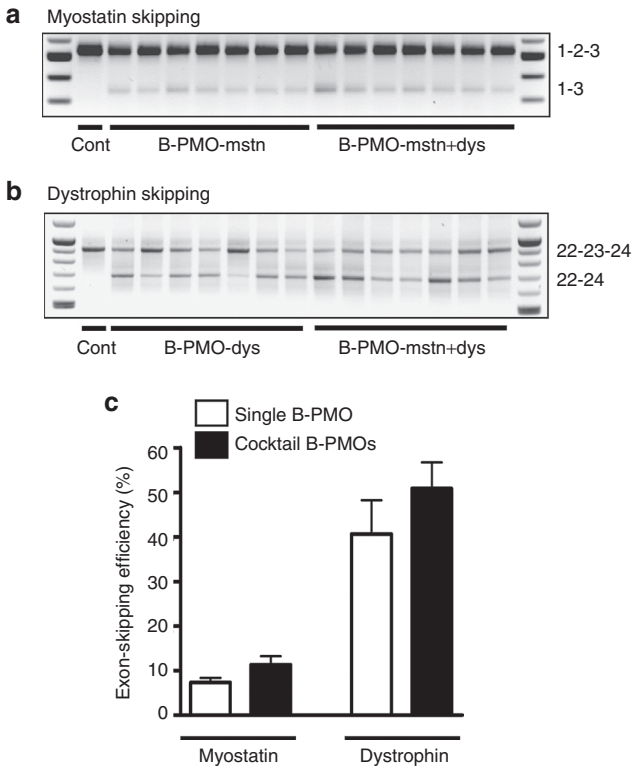

Figure 3 Treatment of *mdx* mouse muscle with B-PMO-mstn and B-PMO-dys induces dual myostatin and dystrophin exon skipping. Skipping of myostatin or dystrophin exons using B-PMOs following single or combined intramuscular injection (10 µg each) into the tibialis anterior (TA) of *mdx* mice. Mice were killed after 8 weeks and a nested RT-PCR was performed in treated and control-injected muscles. (**a**) Representative products of nested RT-PCR analysis of myostatin exon 2 skipping in muscles treated with excipient only (cont), B-PMO-mstn or the cocktail of B-PMO-mstn and B-PMO-dys. (**b**) Representative products of nested RT-PCR analysis of dystrophin exon 23 skipping in muscles treated with excipient only (cont), B-PMO-dys or a cocktail of B-PMO-mstn and B-PMO-dys. (**c**) Densitometric analyses of nested RT-PCR products for percentage of myostatin exon 2, or dystrophin exon 23 skipping in treated and control muscles after individual B-PMO-mstn or B-PMO-dys, or cocktail injection shows that coadministration of the two AOs has no detrimental effect on skipping efficiency. AO, antisense oligonucleotide; PMO, phosphorodiamidate morpholino oligomer; RT-PCR, reverse transcription-PCR.

control. Six mice were killed 1, 2, 4, and 8 weeks after injection, and both TA muscles weighed. Reverse transcription-PCR (RT-PCR) analysis following Vivo-PMO-mstn treatment has shown that skipping the exon 2 of mstn pre-mRNA produces two shorter out-of-frame nonfunctional transcripts. In particular, the upper and lower bands correspond to the complete product including exons 1, 2, and 3 (532 bp) and the exon 2 skipped out-of-frame product (158 bp), respectively. The intermediate out-of-frame product contains a partial sequence of exon 2 due to a cryptic 3′ splice site 296 nt downstream of the correct one.[12] Following intramuscular injection of Vivo-PMO-mstn, myostatin mRNA skipping was observed within 1 week and was still detectable after 8 weeks. The level of skipping as quantified by densitometric analyses remained at high and similar levels for 1 month and thereafter dropped significantly during the second month of the experiment: week 1: 75.1 ± 5.6%; week 2: 65.6 ± 13%; week 4: 74.4 ± 11.5%; week 8: 37.5 ± 4.5% (**Figure 1a,b**). There was no difference in the weight of treated and control TA muscles after week 1 and week 2. However, after 4 weeks, the treated muscles showed a significant increase in weight relative to the control muscle (two-tailed *t*-test, $P = 0.04$, $n = 6$) (**Figure 1c**). After 8 weeks, this response was even more pronounced (two-tailed *t*-test, $P = 0.005$, $n = 6$) (**Figure 1c**). We then compared the distribution of fiber cross-sectional area (CSA) in TA, staining the muscle sections with a laminin antibody. Surprisingly, no significant change in CSA of the muscle fibers was observed (**Supplementary Figure S1**) neither was there any significant change in the number of fibers in treated compared with control muscles. However, even if the muscles of treated mice were no larger than the saline-treated controls in the central region, treated muscles were proximally and distally wider (**Figure 1d**). These data indicate that the 8 weeks timepoint, corresponding to a state when the muscle weight is increasing while the skipping efficiency is dropping, represents

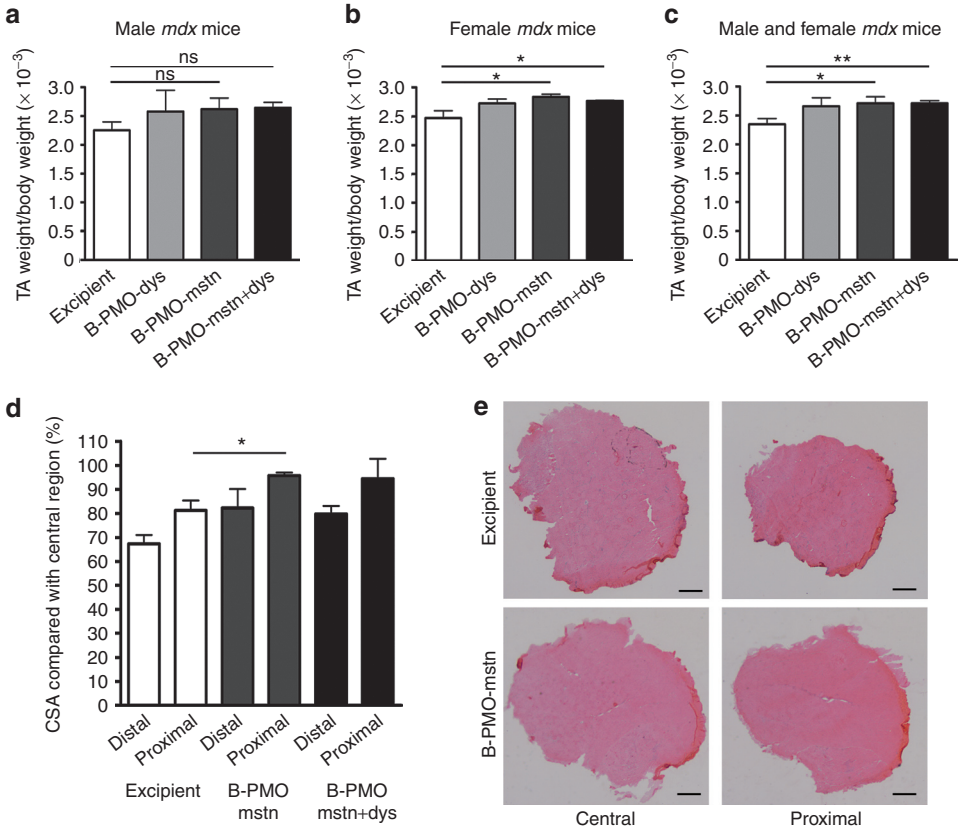

Figure 4 B-PMO-mstn treatment increases the muscle mass in *mdx* mice with or without concurrent B-PMO-dys treatment. Tibialis anterior (TA) muscles treated with a single intramuscular injection of 10 µg B-PMO-dys, 10 µg B-PMO-mstn, 20 µg B-PMO-mstn+dys or excipient were collected and weighed after 8 weeks. (**a**) Mass of TA muscles was unchanged after B-PMO-mstn treatment in male mice (ns = nonsignificant, $n = 4$). (**b**) Treatment with B-PMO-mstn (*$P = 0.048$; $n = 3$) and with B-PMO-mstn+dys (*$P = 0.037$; $n = 4$) induced a significant increase in the weight of muscles of female mice compared with the injection of excipient (two-tailed *t*-test). (**c**) The analysis of combined male and female data from **a** and **b** shows that the treatment with B-PMO-mstn (*$P = 0.03$) and with B-PMO-mstn+dys (**$P = 0.006$) induced a significant increase in weight compared with excipient injection (two-tailed *t*-test, *$P < 0.05$, $n = 7$). (**d**) Treatment with B-PMO-mstn induced a significant increase in CSA of muscle sections harvested from the proximal region of the TA muscles of female *mdx* mice compared with the same sections taken from excipient-injected muscles (two-tailed *t*-test, *$P < 0.05$, $n = 3, 4$ per condition). (**e**) Representative pictures of central and proximal muscle sections from excipient- or B-PMO-mstn–treated muscles of female *mdx* mice. Bar, 300 µm. CSA, cross-sectional area; PMO, phosphorodiamidate morpholino oligomer.

the most convenient time to analyze the effect of the myostatin knockdown in murine skeletal muscles.

Myostatin knockdown after single intramuscular administration of PMO-mstn conjugated to a cell-penetrating peptide (B-PMO-mstn) induces significant increase in muscle mass

Once we have established that Vivo-PMO administration induces a clear increase in muscle mass after 8 weeks, we compared the efficacy of an arginine-rich cell-penetrating peptide-conjugated PMO (B-PMO-mstn) with the Vivo-PMO-mstn at this timepoint by injecting the TA muscles of 6-week-old C57BL10 mice with 10 µg of each compound ($n = 6$). As controls, we used either 10 µg of the unconjugated PMO-mstn, that represents the baseline to quantify the effectiveness of the conjugated moieties,[12] or the same volume of saline. Mice were killed after 8 weeks and TA muscle weighed. Myostatin exon skipping was confirmed at the transcript level in the treated muscles by nested RT-PCR. Densitometric analysis of the skipped and full-length cDNA bands showed that there was 8.9 ± 0.9% myostatin exon 2 skipping with unconjugated PMO, 46.5 ± 2.9% exon skipping with Vivo-PMO-mstn, and 62.5 ± 5.3% exon skipping with B-PMO-mstn (**Figure 2a,b**). There was found to be a significant increase in the weights of TA muscles treated with B-PMO (two-tailed *t*-test, $P = 0.04$, $n = 6$) as well as Vivo-PMO (two-tailed *t*-test, $P = 0.01$, $n = 6$) compared with saline-treated controls (**Figure 2c,d**) while, as expected, unconjugated PMO did not lead to any significant change in the TA weight. Again while the weight and shape was changed, no difference was observed for fiber CSA in B-PMO–treated muscles, and only the TA muscle fibers of Vivo-PMO-mstn–treated animals showed a small but significant shift on the distribution of CSA relative to saline-injected animals (**Supplementary Figure S2a**, $0.04 < P < 0.05$, χ^2 test). Standard hematoxylin and eosin staining showed no major histological changes between controls and treated muscles (**Supplementary Figure S2b**). These data confirmed that the conjugation of PMO-mstn with a cell-penetrating peptide yielded a reagent that induces muscle mass augmentation in wild-type mice following intramuscular injection.

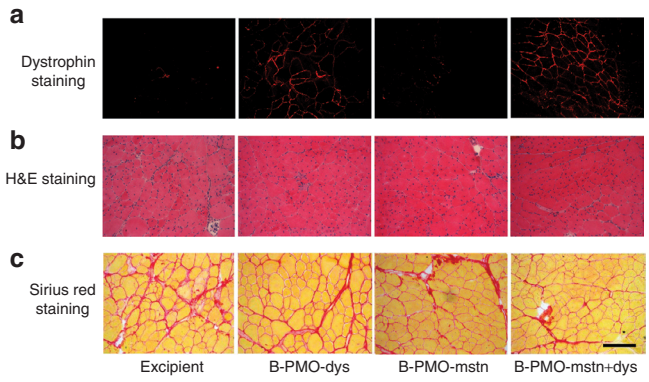

Figure 5 B-PMO-dys– and B-PMO-mstn+dys-treated mdx muscles show substantial dystrophin restoration on the sarcolemma of muscle fibers with no histological hallmarks of toxicity or fibrosis. Tibialis anterior (TA) muscles treated with a single intramuscular injection of 10 µg B-PMO-dys, 10 µg B-PMO-mstn, 20 µg B-PMO-mstn+dys or excipient were cut in transverse sections and (**a**) dystrophin expression and the (**b**) H&E histology of the samples were analyzed. (**a**) Muscles treated with either B-PMO-dys or B-PMO-mstn+dys express dystrophin widely. (**b**) Representative H&E staining of TA muscle cross-sections showed no overt signs of toxic or inflammatory effects as a result of B-PMO injections. (**c**) Representative pictures of Sirius red staining of TA muscle cross-sections showed no overt signs of fibrotic changes associated with B-PMO injections. Bar, 200 µm. H&E, hematoxylin and eosin; PMO, phosphorodiamidate morpholino oligomer.

In vivo coinjection of B-PMO-mstn and a B-PMO–targeting dystrophin transcript reframing in dystrophic muscles induces both dystrophin expression and gender-specific muscle mass augmentation

Dual exon skipping of both myostatin and dystrophin has been recently proposed as possible strategy to ameliorate the dystrophic pathology.[13] We verified the effectiveness of using the cell-penetrating peptide linked to PMO to downregulate both myostatin expression and reframe the dystrophin transcript in *mdx* mice. Whilst for myostatin downregulation we used the B-PMO-mstn, for the skipping of dystrophin we used the B-peptide–conjugated form of the extensively tested 25-mer PMO targeting the 5′ splice site of murine dystrophin intron 23.[16–18] The experiment was performed in both male and female *mdx* mice in order to evaluate a possible gender-specific outcome. TA muscles of 6-week-old *mdx* mice were treated with a single intramuscular injection of 10 µg of B-PMO-dys alone, B-PMO-mstn alone, or a 20 µg cocktail of B-PMO-mstn and B-PMO-dys (B-PMO-mstn+dys). Control muscles were treated with the same volume of excipient. Mice were killed 8 weeks after injection. Efficiency of PMO-induced exon skipping was tested by nested RT-PCR. No significant differences in the exon-skipping efficacy was observed between male and female muscles for myostatin or dystrophin transcripts skipped alone, or in combination. When administered individually, exon skipping was clearly detected at the transcript level in muscles treated with B-PMO-mstn (7.3 ± 0.9, **Figure 3a**) and B-PMO-dys (40.7 ± 7.5%, **Figure 3b**) for myostatin and dystrophin transcripts, respectively. Dual exon skipping of both myostatin exon 2 (11.3 ± 1.9%, **Figure 3a**) and dystrophin exon 23 (50.9 ± 5.9%, **Figure 3b**) induced by treatment of the same muscle with a cocktail of both B-PMO-mstn and B-PMO-dys was also clearly detected by nested RT-PCR, showing that myostatin or dystrophin exon skipping was not detrimentally influenced by the presence of two AOs (**Figure 3e**). Interestingly, while in male and female muscles a similar amount of skipped product was observed, a different outcome in the weight of the dystrophic muscles was found between male and female mice after the injection of B-PMO. In the muscles of treated males, no significant change in muscle weight was observed in TAs treated with B-PMO-mstn alone or B-PMO-mstn+dys compared with saline-treated controls (**Figure 4a**, $n = 3–4$ per condition). On the contrary, in treated muscles of female mice a significant increase in the weights of TAs treated with B-PMO-mstn alone (two-tailed *t*-test, $P = 0.048$) or a cocktail of B-PMO-mstn+dys (two-tailed *t*-test, $P = 0.037$) was found compared with saline-treated controls (**Figure 4b**, $n = 3–4$ per condition). As expected, B-PMO-dys did not lead to any significant change in the TA weight on its own (**Figure 4a,b**). Importantly, the global analysis made from male and female muscles together showed a statistically significant difference in muscles treated with B-PMO-mstn alone (two-tailed *t*-test, $P = 0.03$, $n = 7$) or with the cocktail of B-PMO-mstn+dys (two-tailed *t*-test, $P = 0.006$, $n = 7$) compared with saline controls (**Figure 4c**). Muscle fiber CSA was not affected by the treatments (**Supplementary Figure S3**). However, as we observed in C57BL10 muscles injected with Vivo-PMO-mstn, there were larger proximal and distal circumferences compared with saline-injected muscles. In particular, sections corresponding to the proximal region of B-PMO-mstn–treated muscles were statistically significantly larger than the corresponding sections in excipient-injected muscles (**Figure 4d,e**). No significant difference was observed for distal regions between B-PMOs and excipient-treated muscles in female mice or for proximal or distal and central regions in male muscles (data not shown). Immunofluorescence detection of dystrophin in whole transverse TA muscle sections revealed notably similar dystrophin expression in all B-PMO-dys– and B-PMO-mstn+dys-treated muscles (**Figure 5a**). Importantly, muscles stained for hematoxylin and eosin showed no noticeable damage due to the treatment with B-PMOs when compared with the muscles of saline-treated *mdx* mice (**Figure 5b**). Sirius red staining of muscle sections was performed to evaluate levels of fibrosis but no obvious change was observed in treated muscles compared with the controls (**Figure 5c**). These results demonstrate that the independent myostatin or dystrophin exon-skipping events were not detrimentally influenced by mixing and coadministration of the two AOs. Furthermore, dual myostatin and dystrophin exon skipping induced both muscle augmentation and dystrophin expression.

Discussion

The knockdown of myostatin, a negative regulator of skeletal muscle mass[1] has been proven to efficiently induce skeletal muscle augmentation.[2] We have recently demonstrated that skipping the out-of-frame exon 2 of myostatin from the pre-mRNA with the consequent knockdown of the protein is a feasible method to increase the muscle mass in normal mice.[12] The most obvious approach to ameliorate DMD is to induce the re-expression of dystrophin in the cardiac and skeletal muscles. One of the most promising approaches is based on the use of antisense therapy with PMOs and 2′OMePS

AOs that have been successful on reframing the dystrophin transcript and so restoring dystrophin expression in *mdx* mice[16,19,20] and, most importantly, in humans.[21,22] In this context, AO-mediated myostatin knockdown might be a potential adjunct therapy for DMD with the aim of stimulating the growth of muscle tissue while reducing or reversing the substitution of muscle fibers with fat and fibrotic tissue. Recently the co-delivery of antisense adeno-associated virus (AAV) vectors to induce dystrophin restoration (AAV-U7-DYS) and muscle mass augmentation *via* inhibition of the myostatin receptor, activin receptor IIb (AAV-shAcRIIb) in dystrophic mice has been published.[23] These experiments suggested that downregulation of AcRIIb on its own was not sufficient to improve muscle strength of treated muscles. However, the combined downregulation of AcRIIb and restoration of dystrophin expression led to significant improvements in absolute and specific maximal muscle strength that was better than dystrophin restoration on its own.[23] *In vitro* studies using 2′OMePS AOs showed that myostatin and dystrophin AOs can be used simultaneously to induce exon skipping of pre-mRNAs of both the genes, and most importantly in human DMD cells.[13] Here, we used the PMO chemistry that offers the advantage of being easily conjugated with moieties that improve the efficacy of delivery *in vivo*. Our PMO for myostatin exon 2 skipping was conjugated with an octaguanidine moiety (Vivo-PMO) as previously published[12] or to a cell-penetrating peptide based on L-arginine, 6-aminohexanoic acid, and β-alanine as already described for the exon-skipping approach of the dystrophin gene.[24,25] A single intramuscular treatment of 10 µg of Vivo-PMO resulted in efficient skipping lasting for a month following the injection and dropping during the following month. Myostatin knockdown led to an increase in muscle weight starting 1 month after the injection and increasing during the next 4 weeks. The effect of the myostatin protein knockdown showed a delayed effect on the muscle compared with the transcript reframing. To our knowledge, a direct comparison between Vivo-PMO and B-PMO efficiency has not been performed to date. Here, we show that for myostatin exon skipping, Vivo-PMO proved to be superior than B-PMO in normal mice in that Vivo-PMO–treated muscles were heavier and showed a small but detectable change in the distribution of the fiber CSA. However, B-PMO induced more transcript reframing and the effect of B-PMO-mstn on the muscle weight may have been simply delayed. B-PMO-mstn induced higher skipping efficiency of myostatin in wild-type (62.5%) compared with *mdx* (7.3%) mice. We do not have an explanation for this latter difference in skipping efficiency. However, it is possible that the pseudohypertrophic mdx muscles and the concurrent lower amount of myostatin transcript expressed[26] could reduce the efficacy of PMO activity, compared with wild-type muscles. Simultaneously, intramuscular B-PMO treatment targeting myostatin and dystrophin resulted in significant muscle mass augmentation and dystrophin expression. The use of a cocktail of B-PMOs had no effect on the levels of myostatin skipping seen compared with use of the myostatin B-PMO alone. Our findings suggest that the AOs used for reframing myostatin and dystrophin transcript did not have a detrimental interaction thus confirming findings from another group.[13] B-PMO administered in muscles of male *mdx* mice did not achieve a significant change in muscle mass while in female mice muscle augmentation was statistically significant. Muscles of either female or male wild-type mice have no difference in the amount of expressed mRNA or in the unprocessed full-length myostatin protein. However, in female mice a post-translational increase of processed, bioactive myostatin has been measured compared with male muscles which may account for the different muscle size.[27] In contrast, in different muscles of *mdx* mice there seems to be variability in myostatin expression.[28] However, no studies have been performed to clarify whether TA muscles of *mdx* mice show gender-specific differences in myostatin expression. A possible explanation of the gender-specific difference observed in our study is that the hypertrophic effect induced by our dose regimen of B-PMO-mstn was still not efficient enough to be observed in the pseudohypertrophic mdx male muscles. The smaller muscles of female mdx mice, containing supposedly less myostatin, may show a much clearer effect. However, a better understanding of how a combination of myostatin inhibition and dystrophin expression restoration affects force generation, resistance to eccentric contraction, and other functional, contractile properties of the treated muscles is needed. Nevertheless, our data indicate that myostatin exon skipping alongside dystrophin expression restoration shows significant potential to be a part of a dual antisense combination therapy to counter dystrophin deficiency and its consequences in DMD.

Materials and Methods

Animal studies and PMO administration. For the *in vivo* experiments with C57BL10 mice, animals were bought from Harlan (Blacktown, UK). For mdx experiments, animals were bred in-house and food and water provided *ad libitum*. *In vivo* experimentation was conducted under statutory Home Office recommendation, regulatory, ethical, and licensing procedures and under the Animals (Scientific Procedures) Act 1986 (project licences PPL 70/7008 and 30/2652). Vivo-PMOs were obtained from Gene Tools (Philomath, OR). B-PMOs were synthesized as previously stated.[25] The sequences of PMO-mstn and PMO-dys were 5′-AGCCCATCTTCTCCTG-GTCCTGGGAAGG-3′ and 5′-GGCCAAACCTCGGCTTACC TGAAAT-3′, respectively.[18,29] The desired dilutions of the AOs were prepared in 30 µl of sterile injectable saline or sterile 5% glucose solution depending on the experiment. Animals were anesthetized *via* intraperitoneal injection of 3 µl/g body weight of 25% (vol/vol) fentanyl/fluanisone (Hypnorm) and 25% (vol/vol) midazolam (Hypnovel) in sterile water or with isofluorane gas; intramuscular injections were made into TA muscles. During recovery, the animals were placed on a heating pad and monitored hourly for about 4 hours. For relevant experiments, whole body weights were recorded weekly. TAs of treated and control mice were excised postmortem and weights were recorded. To calculate the variation in muscle weight, TA weights were normalized against the whole body weight for each individual animal. The muscles were embedded in OCT embedding medium and frozen in isopentane cooled with liquid nitrogen.

RNA isolation and RT-PCR. RNA was extracted from blocks using TRIzol reagent (Invitrogen, Scotland, UK). RNA was then extracted from the homogenized samples by using the

manufacturer's instructions; 1 µg of RNA was reverse transcribed and resulting cDNA amplified using specific primers; 1 µl of PCR products obtained was used as a template for carrying out nested PCR using a second set of primers (MWG, Ebersberg, Germany). Nested PCR products were loaded in 1.2% agarose gels. PCR programs and primer sequences are available on request. Densitometric analysis of the gels was performed using Gene tools 3.05 (Syngene, Cambridge, UK).

Muscle sectioning, immunofluorescence, and histological staining. Cryosectioning was performed with OTF 5000 cryostat (Bright, Huntingdon, UK) and 10 µm transverse sections of each muscle were cut at up to 10 levels through the muscle length. The tissue cut in the intervening sections between the levels of a block was collected in precooled 1.5 ml eppendorf tubes for RNA extraction and stored at –80 °C. For laminin staining, slides were fixed with ice-cold acetone and then blocked with 5% milk in phosphate-buffered saline with Tween 20 (PBST). Primary antibody solution was a rat anti-laminin antibody (L9393; Sigma-Aldrich, Poole, UK) diluted to 1:1,000 in 2.5% milk in PBST. Secondary antibody was an anti-rat biotinylated (Vector laboratories, Burlingame, CA). Alexafluor Streptavidin-568 (S-11226; Invitrogen) diluted to 1:1,000 in 2.5% milk in PBST was finally added to the slides. Slides were finally mounted in vectashield, hard set mounting medium for fluorescence with DAPI (4′,6-diamidino-2-phenylindole). For dystrophin staining, the same protocol was used but the primary antibody used was H12 Polyclonal rabbit antibody[30] diluted to 1:100 in 2.5% milk in PBST. The secondary antibody Alexafluor goat anti-rabbit-568 (A-11011; Invitrogen), diluted to 1:200 in 2.5% milk in PBST was added.

Histological and morphometric analyses. Muscle size was estimated in muscle sections previously stained for hematoxylin and eosin by using a standard protocol. A laminin staining was used to analyze the muscle fiber size. CSA for the whole muscle fibers were measured using SigmaScan Pro 5.0.0 (Systat Software, London, UK). Fibrosis was evaluated in muscle sections stained with Sirius red following a standard protocol.

Statistical analysis. Data are expressed as mean ± SEM. Student's two-tailed *t*-test and χ^2 test were used for the analyses. P values <0.05 were considered significant ($^*P < 0.05$, $^{**}P < 0.01$, $^{***}P < 0.001$). For all statistical analyses, GraphPad Prism software package (version 4; GraphPad Software, La Jolla, CA) was used.

Supplementary Material

Figure S1. Distribution of cross-sectional area (CSA) of muscle fibers in Vivo-PMO–treated (black bars) TA muscles shows no difference with the saline-injected (white bars) TA muscles 4 ($P > 0.7$) or 8 ($P > 0.9$) weeks after the injection (χ^2 test, $n = 6$).
Figure S2. C57BL10 TA muscles were injected with unconjugated PMO-mstn, Vivo-PMO-mstn or B-PMO-mstn and mice were killed 8 weeks after the injection.
Figure S3. CSA distribution in TA muscles of *mdx* mice treated with 10 µg of B-PMO-mstn, B-PMO-dys or a cocktail of B-PMO-mstn+dys.

Acknowledgments. All authors contributed to the interpretation of results and drafting of the report and have seen and approved the final version. *In vivo* experimental work was planned and conducted by A.M., J.K.K., G.M., M.J.A.W., and G.D. B-PMO reagents were designed by L.P. and G.D. and produced by A.F.S. and M.J.G. M.J.G., M.J.A.W., and G.D. supervised design, management, and analyses of the study. This research work was supported by funds from the Muscular Dystrophy Campaign (MDC UK), the EU Clinigene Network of Excellence (LSHB-CT-2006-018933), and the Association Française contre les Myopathies (AFM). The academic support of the MDEX Consortium (http://www.mdex.org.uk/) and the EU TREAT-NMD Network of Excellence (LSHM-CT-2006-036825) are also acknowledged. The authors declared no conflict of interest.

1. Carnac, G, Ricaud, S, Vernus, B and Bonnieu, A (2006). Myostatin: biology and clinical relevance. *Mini Rev Med Chem* **6**: 765–770.
2. Patel, K and Amthor, H (2005). The function of Myostatin and strategies of Myostatin blockade-new hope for therapies aimed at promoting growth of skeletal muscle. *Neuromuscul Disord* **15**: 117–126.
3. Whittemore, LA, Song, K, Li, X, Aghajanian, J, Davies, M, Girgenrath, S et al. (2003). Inhibition of myostatin in adult mice increases skeletal muscle mass and strength. *Biochem Biophys Res Commun* **300**: 965–971.
4. Wagner, KR, Fleckenstein, JL, Amato, AA, Barohn, RJ, Bushby, K, Escolar, DM et al. (2008). A phase I/IItrial of MYO-029 in adult subjects with muscular dystrophy. *Ann Neurol* **63**: 561–571.
5. Wolfman, NM, McPherron, AC, Pappano, WN, Davies, MV, Song, K, Tomkinson, KN et al. (2003). Activation of latent myostatin by the BMP-1/tolloid family of metalloproteinases. *Proc Natl Acad Sci USA* **100**: 15842–15846.
6. Foster, K, Graham, IR, Otto, A, Foster, H, Trollet, C, Yaworsky, PJ et al. (2009). Adeno-associated virus-8-mediated intravenous transfer of myostatin propeptide leads to systemic functional improvements of slow but not fast muscle. *Rejuvenation Res* **12**: 85–94.
7. Lee, SJ and McPherron, AC (2001). Regulation of myostatin activity and muscle growth. *Proc Natl Acad Sci USA* **98**: 9306–9311.
8. Cadena, SM, Tomkinson, KN, Monnell, TE, Spaits, MS, Kumar, R, Underwood, KW et al. (2010). Administration of a soluble activin type IIB receptor promotes skeletal muscle growth independent of fiber type. *J Appl Physiol* **109**: 635–642.
9. Amantana, A and Iversen, PL (2005). Pharmacokinetics and biodistribution of phosphorodiamidate morpholino antisense oligomers. *Curr Opin Pharmacol* **5**: 550–555.
10. Malerba, A, Thorogood, FC, Dickson, G and Graham, IR (2009). Dosing regimen has a significant impact on the efficiency of morpholino oligomer-induced exon skipping in mdx mice. *Hum Gene Ther* **20**: 955–965.
11. Arora, V, Devi, GR and Iversen, PL (2004). Neutrally charged phosphorodiamidate morpholino antisense oligomers: uptake, efficacy and pharmacokinetics. *Curr Pharm Biotechnol* **5**: 431–439.
12. Kang, JK, Malerba, A, Popplewell, L, Foster, K and Dickson, G (2011). Antisense-induced myostatin exon skipping leads to muscle hypertrophy in mice following octa-guanidine morpholino oligomer treatment. *Mol Ther* **19**: 159–164.
13. Kemaladewi, DU, Hoogaars, WM, van Heiningen, SH, Terlouw, S, de Gorter, DJ, den Dunnen, JT et al. (2011). Dual exon skipping in myostatin and dystrophin for Duchenne muscular dystrophy. *BMC Med Genomics* **4**: 36.
14. Heemskerk, HA, de Winter, CL, de Kimpe, SJ, van Kuik-Romeijn, P, Heuvelmans, N, Platenburg, GJ et al. (2009). In vivo comparison of 2'-O-methyl phosphorothioate and morpholino antisense oligonucleotides for Duchenne muscular dystrophy exon skipping. *J Gene Med* **11**: 257–266.
15. Yin, H, Moulton, HM, Seow, Y, Boyd, C, Boutilier, J, Iverson, P et al. (2008). Cell-penetrating peptide-conjugated antisense oligonucleotides restore systemic muscle and cardiac dystrophin expression and function. *Hum Mol Genet* **17**: 3909–3918.
16. Alter, J, Lou, F, Rabinowitz, A, Yin, H, Rosenfeld, J, Wilton, SD et al. (2006). Systemic delivery of morpholino oligonucleotide restores dystrophin expression bodywide and improves dystrophic pathology. *Nat Med* **12**: 175–177.
17. Fletcher, S, Honeyman, K, Fall, AM, Harding, PL, Johnsen, RD and Wilton, SD (2006). Dystrophin expression in the mdx mouse after localised and systemic administration of a morpholino antisense oligonucleotide. *J Gene Med* **8**: 207–216.
18. Gebski, BL, Mann, CJ, Fletcher, S and Wilton, SD (2003). Morpholino antisense oligonucleotide induced dystrophin exon 23 skipping in mdx mouse muscle. *Hum Mol Genet* **12**: 1801–1811.
19. Lu, QL, Rabinowitz, A, Chen, YC, Yokota, T, Yin, H, Alter, J et al. (2005). Systemic delivery of antisense oligoribonucleotide restores dystrophin expression in body-wide skeletal muscles. *Proc Natl Acad Sci USA* **102**: 198–203.

20. Malerba, A, Sharp, PS, Graham, IR, Arechavala-Gomeza, V, Foster, K, Muntoni, F et al. (2011). Chronic systemic therapy with low-dose morpholino oligomers ameliorates the pathology and normalizes locomotor behavior in mdx mice. *Mol Ther* **19**: 345–354.
21. Cirak, S, Arechavala-Gomeza, V, Guglieri, M, Feng, L, Torelli, S, Anthony, K et al. (2011). Exon skipping and dystrophin restoration in patients with Duchenne muscular dystrophy after systemic phosphorodiamidate morpholino oligomer treatment: an open-label, phase 2, dose-escalation study. *Lancet* **378**: 595–605.
22. Goemans, NM, Tulinius, M, van den Akker, JT, Burm, BE, Ekhart, PF, Heuvelmans, N et al. (2011). Systemic administration of PRO051 in Duchenne's muscular dystrophy. *N Engl J Med* **364**: 1513–1522.
23. Dumonceaux, J, Marie, S, Beley, C, Trollet, C, Vignaud, A, Ferry, A et al. (2010). Combination of myostatin pathway interference and dystrophin rescue enhances tetanic and specific force in dystrophic mdx mice. *Mol Ther* **18**: 881–887.
24. Yin, H, Lu, Q and Wood, M (2008). Effective exon skipping and restoration of dystrophin expression by peptide nucleic acid antisense oligonucleotides in mdx mice. *Mol Ther* **16**: 38–45.
25. Betts, C, Saleh, AF, Arzumanov, AA, Hammond, SM, Godfrey, C, Coursindel, T et al. (2012). Pip6-PMO, a new generation of peptide-oligonucleotide conjugates with improved cardiac exon skipping activity for DMD treatment. *Mol Ther Nucleic Acids* **1**: e38.
26. Zhu, X, Hadhazy, M, Wehling, M, Tidball, JG and McNally, EM (2000). Dominant negative myostatin produces hypertrophy without hyperplasia in muscle. *FEBS Lett* **474**: 71–75.
27. McMahon, CD, Popovic, L, Jeanplong, F, Oldham, JM, Kirk, SP, Osepchook, CC et al. (2003). Sexual dimorphism is associated with decreased expression of processed myostatin in males. *Am J Physiol Endocrinol Metab* **284**: E377–E381.
28. Spassov, A, Gredes, T, Gedrange, T, Lucke, S, Pavlovic, D and Kunert-Keil, C (2011). The expression of myogenic regulatory factors and muscle growth factors in the masticatory muscles of dystrophin-deficient (mdx) mice. *Cell Mol Biol Lett* **16**: 214–225.
29. Kang, JK, Malerba, A, Popplewell, L, Foster, K and Dickson, G (2011). Antisense-induced myostatin exon skipping leads to muscle hypertrophy in mice following octa-guanidine morpholino oligomer treatment. *Mol Ther* **19**: 159–164.
30. Sherratt, TG, Vulliamy, T and Strong, PN (1992). Evolutionary conservation of the dystrophin central rod domain. *Biochem J* **287 (Pt 3)**: 755–759.

Supplementary Information accompanies this paper on the Molecular Therapy–Nucleic Acids website (http://www.nature.com/mtna)